Available online at www.sciencedirect.com

SciVerse ScienceDirect

Ceramics International 39 (2013) 1359–1363

CERAMICS INTERNATIONAL

www.elsevier.com/locate/ceramint

Characteristics of highly (001) oriented (K,Na)NbO_3 films grown on $LaNiO_3$ bottom electrodes by RF magnetron sputtering

Tao Li[a], Genshui Wang[a], Denis Remiens[b], Xianlin Dong[a,*]

[a]*Key Laboratory of Inorganic Functional Materials and Devices, Shanghai Institute of Ceramics, Chinese Academy of Sciences, 1295 Dingxi Road, Shanghai 200050, People's Republic of China*

[b]*IEMN-DOAE, CNRS UMR 8520, Cité scientifique, 59655 Villeneuve-d'Ascq Cedex, France*

Received 25 May 2012; received in revised form 21 July 2012; accepted 21 July 2012
Available online 4 August 2012

Abstract

(K,Na)NbO_3 ferroelectric films were grown on $LaNiO_3$ coated silicon substrates by RF magnetron sputtering. The conductive $LaNiO_3$ films acted as seed layers and induced the highly (001) oriented perovskite (K,Na)NbO_3 films. Such films exhibit saturated hysteresis loops and have a remnant polarization ($2P_r$) of 23 μC/cm^2, and coercive field ($2E_c$) of 139 kV/cm. The films showed a fatigue-free behavior up to 10^9 switching cycles. A high tunability of 65.7% (@300 kV/cm) was obtained in the films. The leakage current density of the films is about 6.0×10^{-8} A/cm^2 at an electric field of 50 kV/cm.

Keywords: C. Ferroelectric; (K,Na)NbO_3; $LaNiO_3$; Thin films

1. Introduction

In the past decade, lead-free piezoelectric ceramics have received considerable attention due to the toxicity of lead-based piezoelectric ceramics. $(K_{0.5}Na_{0.5})NbO_3$ (abbreviated as KNN) is a promising candidate for lead-free piezoelectric material owing to its high Curie temperature and excellent piezoelectric properties [1–3]. Driven by the miniaturization and integration [4,5], great effects have been made to fabricate high-quality KNN or KNN-based thin films using different growth techniques, such as chemical solution deposition (CSD) [6], sol–gel deposition [7–9], pulsed laser deposition (PLD) [10–12], and RF magnetron sputtering [13–18]. Among them, RF magnetron sputtering is an attractive technique for applications since deposition can be employed over large area substrates and this technique is commonly used in microelectronic manufactures.

Various types of substrates were used to grow KNN films by sputtering. Wang et al. and Blomqvist et al. grew *c*-axis oriented KNN films on $LaAlO_3$ single crystal substrates and studied the tunability and the dielectric properties of the films [13,17]. High-quality epitaxial KNN films on Pt/MgO and polycrystalline KNN films with a preferential (001) orientation on Pt/Ti/SiO_2/Si were fabricated by Shibata et al. [16]. Wu et al. deposited KNN thin films on the $SrRuO_3$/$SrTiO_3$ substrate and observed a strong (100) preferred orientation [18]. Compared with Pt, $Pt_{80}Ir_{20}$, RuO_2 and $SrRuO_3$, $LaNiO_3$ (LNO) is low cost and can be easily textured without single crystal substrates. In addition, as a typical conductive oxide, its lattice constant $a=3.84$ Å matches well with that of many ferroelectric perovskite oxides [19]. Therefore, it has been used as bottom electrode to improve the structural and electric properties of ferroelectric thin films [20–23]. To our best knowledge, there are no reports on the properties of KNN thin films grown on LNO bottom electrodes. In this study, highly (001) oriented KNN thin films on LNO bottom electrodes were fabricated by the RF magnetron sputtering. The microstructure and the electrical properties of the KNN/LNO/Si films were characterized.

2. Experiment

LNO bottom electrodes were deposited by RF magnetron sputtering on silicon at 450 °C, and then in-situ annealed at 600 °C for 1 h. The LNO film with thickness of 63.5 nm

*Corresponding author.
E-mail address: xldong@sunm.shcnc.ac.cn (X. Dong).

0272-8842/$ - see front matter © 2012 Elsevier Ltd and Techna Group S.r.l. All rights reserved.
http://dx.doi.org/10.1016/j.ceramint.2012.07.074

presented a strong (100) orientation. KNN thin films were deposited on LNO/Si substrates using a 5% mol K,Na-enriched $(K_{0.55}Na_{0.55})NbO_3$ ceramic target, which was synthesized by a conventional solid state reaction route. During the deposition, the substrate temperature was kept at 550 °C, the total pressure was 1.3 Pa with mixed Ar/O_2. After sputtering for 2 h, the KNN thin films were post-annealed at 750 °C for 1 h in an oxygen atmosphere by rapid thermal annealing. The thickness of KNN thin film was 601 nm. To investigate the electrical behavior, circular Pt top electrodes with diameter of 0.15 mm were deposited by sputtering, and then post-annealed at 500 °C for 30 min by conventional thermal annealing.

X-ray diffraction (XRD) with Cu K_α was performed to reveal the structure of the thin film using a Rigaku D/max 2550 V instrument. The surface and cross morphology of the thin films was studied by field emission scanning electron microscope (SEM) (HITACHI S4800). Energy dispersive spectroscopy (EDS) was used to analyze the chemical composition of the thin films. Relative permittivity vs. voltage characteristics were acquired using HP4192A (Agilent Technologies, Santa Clara, CA). Polarization–field (P–E) hysteresis loops of the films were measured by TF analyzer 2000. The leakage current behaviors were characterized by using an electrometer (Keithley 6517A).

3. Results and discussion

Fig. 1 illustrates the XRD-pattern of the KNN film deposited on a LNO/Si substrate. The KNN film is a single phase with preferential (001) orientation, which indicates that the film has its c-axis normal to the substrate surface. The preferential growth was induced by the (001)-oriented LNO buffer layer. The inset of Fig. 1 shows the XRD-pattern of $(K,Na)NbO_3$ ceramic target with $a=3.9266$ Å, $b=3.9664$ Å and $c=3.9844$ Å, which is fitted to the orthorhombic structure. From the observed Bragg reflections in Fig. 1, we can only calculate the out-of-plane parameter of the KNN thin film. The parameter of the KNN film is $c=4.0058$ Å, which is larger than that of the bulk ceramic. This may be attributed to the large lattice misfit of ~4.1% between KNN and LNO. Due to the large lattice mismatch, KNN films experience in-plane compressive stress and appear to be tetragonal out-of-plane distorted.

Surface and cross-sectional SEM images of KNN films are presented in Fig. 2. The surface image showed that the thin film is textured with mean grain sizes of 50–100 nm. It is noted that the textured thin film possesses quadrangular grains, some of which are overlapped and with their special planes parallel to the surface of the thin film. The cross-sectional image indicates that the thin film possesses a dense and columnar microstructure. The thickness of LNO and KNN are estimated to be 63 nm and 601 nm, respectively. EDS was employed to investigate the composition of the target and the thin film. The (K + Na)/Nb ratios of the target and the thin film are 1.007 and 0.98, indicating the loss of monovalent elements in the sputtering process. The Na/(K + Na) ratios of the target and the thin film are 0.45 and 0.46, respectively, which reveals that the ratio of Na/K in the thin film is approximately equal to that in the target.

The variations of the polarization with electric field at room temperature are shown in Fig. 3. Saturated P–E hysteresis loops were obtained at the applied electric field of 400 kV/cm. The remnant polarization ($2P_r$) and the coercive field ($2E_c$) are 23 μC/cm^2 and 139 kV/cm,

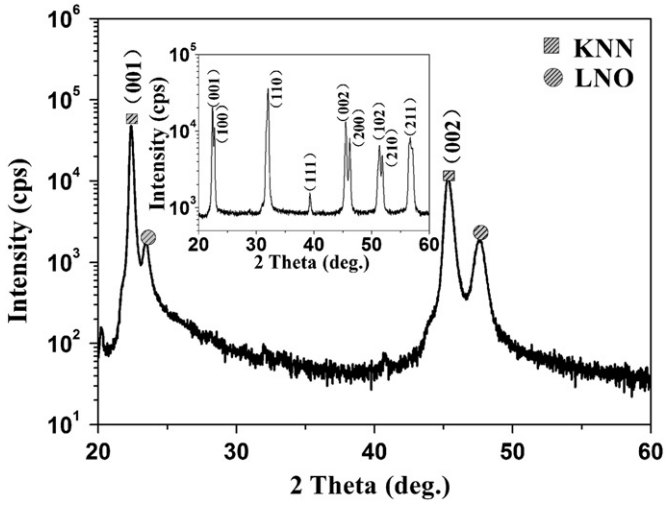

Fig. 1. X-ray diffraction patterns of the KNN/LNO films. Inset shows the XRD pattern of bulk KNN ceramics.

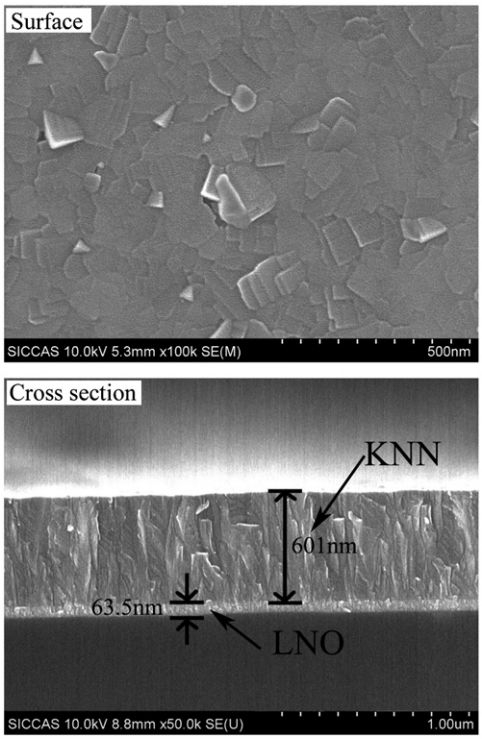

Fig. 2. (a) SEM surface image and (b) SEM cross-sectional image of KNN/LNO films.

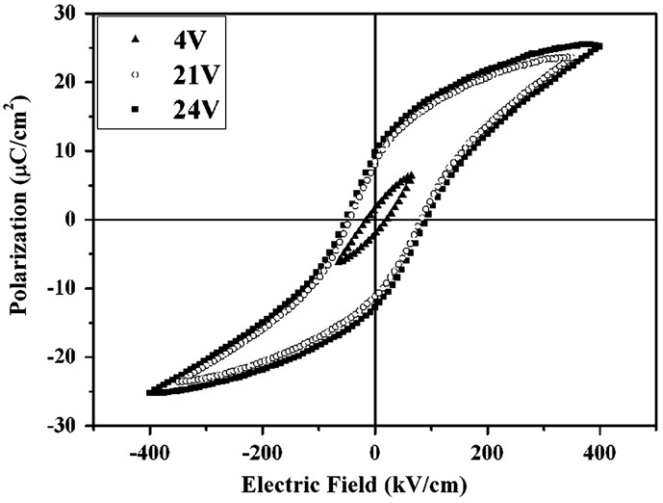

Fig. 3. *P–E* hysteresis loops of Pt/KNN/LNO at room temperature applied with various electrical fields.

respectively. This result is comparable to the value $2P_r = 24$ μC/cm^2 for the epitaxial KNN thin film deposited on $SrRuO_3/SrTiO_3(100)$ substrate [18]. The electrical fatigue characteristics of the KNN thin film is displayed in Fig. 4(a). The measurement was taken at a frequency of 1 MHz. The KNN/LNO/Si film appears fatigue-free subjected to the 10^9 switching cycles, only little polarization degradation is observed, which is similar to other oxide bottom electrodes in improving the fatigue characteristics of the ferroelectric thin films. The fatigue improvement of KNN thin film is thought to be related to the consumption of oxygen vacancies by LNO at the film–electrode interface during cycling [20,21]. Fig. 4(b) shows the *P–E* hysteresis loops before and after the electrical fatigue test. It is noticed that the remnant polarization of KNN films decreased slightly. An asymmetric polarization loop and an internal bias field of $E_i = 12.1$ kV/cm were obtained in the fatigued film. This may be concerned with the trapping electric charges due to the different work-functions between Pt and LNO electrodes during cycling. Besides, the relaxation of stress at the external field can also affect the internal bias field.

Fig. 5 shows the evolution of the relative permittivity and loss tangent of Pt/KNN/LNO as a function of DC bias electric field, applied with an AC small-signal (100 KHz–500 mV) voltage. The ε–V curve displays a butterfly shape, which is typical for a ferroelectric capacitor. The relative permittivity and the loss tangent are 551 and 0.03 at 0 kV/cm, respectively. The Pt/KNN/LNO showed a high tunability of 66% (@300 kV/cm) and a loss tangent of 0.03 at room temperature. The value of 66% is high for KNN films, and is comparable to those of $(Ba,Sr)TiO_3$ and $Pb(Sr,Ti)O_3$ films [24,25], which are popular materials used in tunable applications.

Fig. 6 shows the leakage behavior of Pt/KNN/LNO. The leakage currents were measured with a voltage step of 0.5 V, a step duration of 10 s. It is common that the use of oxide electrodes can result in the increase of the leakage

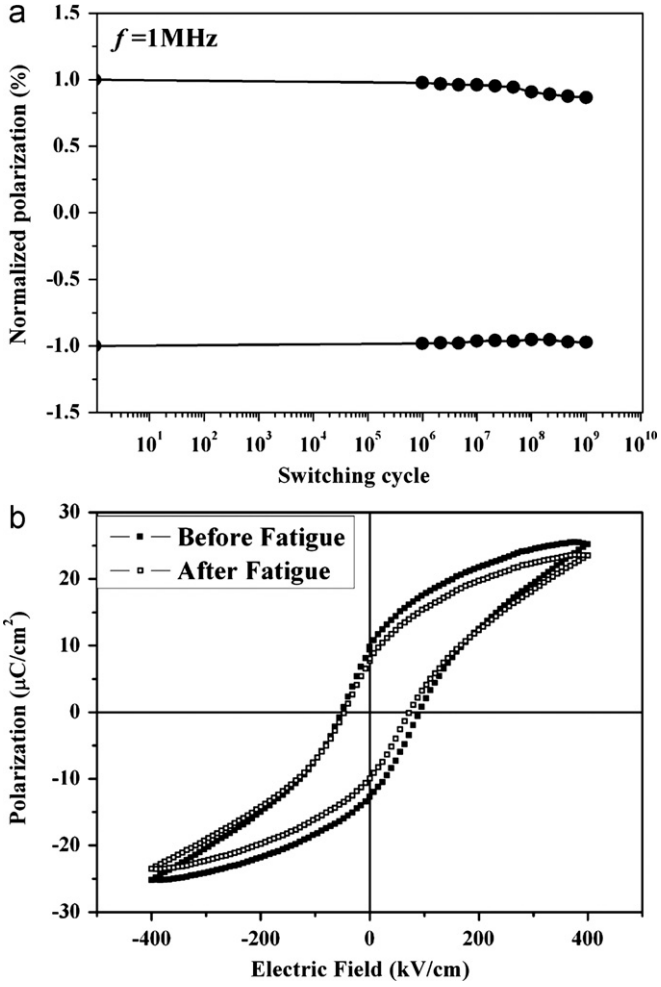

Fig. 4. (a) Fatigue behavior of Pt/KNN/LNO. (b) *P–E* loops of Pt/KNN/LNO before and after fatigue.

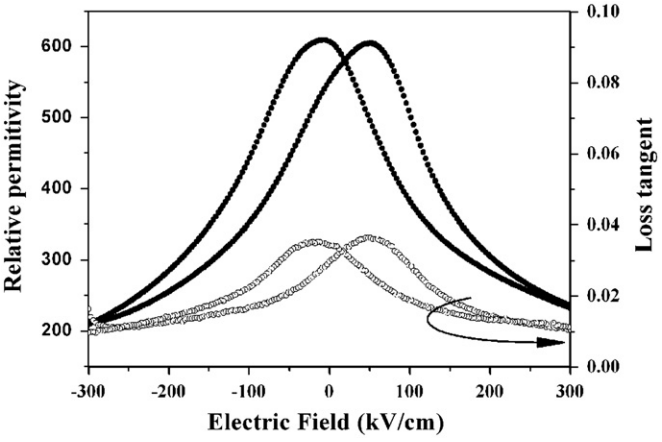

Fig. 5. *E* and tan δ–*E* curves for Pt/KNN/LNO at an applied electrical field of 300 kV/cm.

current density in films, compared with that of metal Pt. For example, the leakage current density of KNN/SRO reported by Wu et al. is in the magnitude of 10^{-6} A/cm^2 at an electric field of 50 kV/cm at room temperature [18], while it is in the magnitude of 10^{-7} A/cm^2 for KNN/Pt [9].

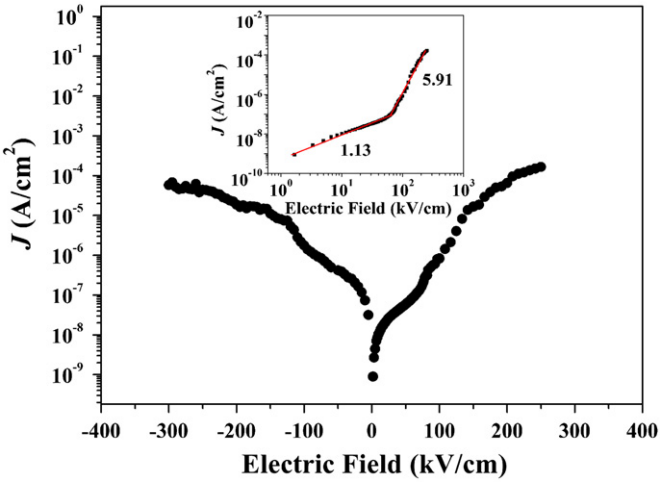

Fig. 6. Leakage current density as a function of applied field for Pt/KNN/LNO. Inset shows the logarithmic plots of dependence of J as a function of E for Pt/KNN/LNO under positive electric field.

In addition, in interdigital capacitors, Blomqvist et al. reported that the leakage current of KNN films is 3.0×10^{-8} A/cm^2 at an electric field of 400 kV/cm [13], which indicates the extremely high intrinsic electric properties in the films. However, the leakage current density of Pt/KNN/LNO in this work is about 6.0×10^{-8} A/cm^2 at an electric field of 50 kV/cm at room temperature, it is even lower than KNN/Pt, which indicates a good state of interface between LNO bottom electrode and KNN films. The inset of Fig. 6 shows the logarithmic plots of dependence of J as a function of E for Pt/KNN/LNO under positive electric field. The J–E curves can be described on the basis of the space charge-limited current (SCLC) model. It was observed that Pt/KNN/LNO follows an Ohmic conduction ($J\sim E^{\alpha}$, $\alpha\sim1$) mechanism in the low electrical field region ($E<68.5$ kV/cm), and SCLC conduction ($J\sim E^{\alpha}$, $\alpha>1$) in the high electrical field ($E>68.5$ kV/cm).

4. Conclusions

In conclusion, KNN films with highly (001) orientations have been deposited on LNO/Si substrates by RF magnetron sputtering. Saturated P–E hysteresis loops with remnant polarization ($2P_r$) and coercive field ($2e_c$) of 23 μC/cm^2 and 139 kV/cm were obtained. The films are almost fatigue-free subjected to 10^9 switching cycles. The tunability of the films was measured to be 66% (@300 kV/cm) and the loss tangent was 0.03. Due to the good state of interface between LNO and KNN, the leakage current density is very low at room temperature. As a result, LNO is a good candidate of bottom electrode material to grow epitaxial KNN films with good electrical properties.

Acknowledgments

This work was supported by the National important basic research project (2012CB619406), Shanghai Basic research project (10DJ1400203), and National Natural Science Foundation of China (No. 10974216).

References

[1] M.D. Maeder, D. Damjanovic, N. Setter, Lead free piezoelectric materials, Journal of Electroceramics 13 (1) (2004) 385–392.
[2] J. Rödel, W. Jo, K.T.P. Seifert, E.-M. Anton, T. Granzow, D. Damjanovic, Perspective on the development of lead-free piezoceramics, Journal of the American Ceramic Society 92 (6) (2009) 1153–1177.
[3] Y. Saito, H. Takao, T. Tani, T. Nonoyama, K. Takatori, T. Homma, T. Nagaya, M. Nakamura, Lead-free piezoceramics, Nature 432 (7013) (2004) 84–87.
[4] N. Setter, D. Damjanovic, L. Eng, G. Fox, S. Gevorgian, S. Hong, A. Kingon, H. Kohlstedt, N.Y. Park, G.B. Stephenson, I. Stolitchnov, A.K. Taganstev, D.V. Taylor, T. Yamada, S. Streiffer, Ferroelectric thin films: review of materials, properties, and applications, Journal of Applied Physics 100 (5) (2006) 051606.
[5] S. Trolier-McKinstry, P. Muralt, Thin film piezoelectrics for MEMS, Journal of Electroceramics 12 (1–2) (2004) 7–17.
[6] C.W. Ahn, E.D. Jeong, S.Y. Lee, H.J. Lee, S.H. Kang, I.W. Kim, Enhanced ferroelectric properties of $LiNbO_3$ substituted $Na_{0.5}K_{0.5}NbO_3$ lead-free thin films grown by chemical solution deposition, Applied Physics Letters 93 (21) (2008) 212905.
[7] P.C. Goh, K. Yao, Z. Chen, Lead-free piezoelectric $(K_{0.5}Na_{0.5})NbO_3$ thin films derived from chemical solution modified with stabilizing agents, Applied Physics Letters 97 (10) (2010) 102901.
[8] A. Chowdhury, J. Bould, M.G.S. Londesborough, S.J. Milne, Fundamental issues in the synthesis of ferroelectric $Na_{0.5}K_{0.5}NbO_3$ thin films by sol–gel processing, Chemistry of Materials 22 (13) (2010) 3862–3874.
[9] F.P. Lai, J.F. Li, Z.X. Zhu, Y. Xu, Influence of Li content on electrical properties of highly piezoelectric (Li, K, Na)NbO_3 thin films prepared by sol–gel processing, Journal of Applied Physics 106 (6) (2009) 064101.
[10] C.R. Cho, A. Grishin, Background oxygen effects on pulsed laser deposited $Na_{0.5}K_{0.5}NbO_3$ films: from superparaelectric state to ferroelectricity, Journal of Applied Physics 87 (9) (2000) 4439–4448.
[11] S. Yamazoe, Y. Miyoshi, K. Komaki, H. Adachi, T. Wada, Ferroelectric properties of $(Na_{0.5}K_{0.5})\cdot NbO_3$ based thin films deposited on Pt/(001)MgO substrate by pulsed laser deposition with $NaNbO_3$ buffer layer, Japanese Journal of Applied Physics 48 (9) (2009) 09KA13.
[12] C.-R. Cho, A. Grishin, Self-assembling ferroelectric $Na_{0.5}K_{0.5}NbO_3$ thin films by pulsed-laser deposition, Applied Physics Letters 75 (2) (1999) 268–270.
[13] M. Blomqvist, J.H. Koh, S. Khartsev, A. Grishin, J. Andreasson, High-performance epitaxial $Na_{0.5}K_{0.5}NbO_3$ thin films by magnetron sputtering, Applied Physics Letters 81 (2) (2002) 337–339.
[14] S. Khartsev, A. Grishin, J. Andreasson, J.H. Koh, J.S. Song, Comparative characteristics of $Na_{0.5}K_{0.5}NbO_3$ films on Pt by pulsed laser deposition and magnetron sputtering, Integrated Ferroelectrics 55 (1) (2003) 769–779.
[15] H.J. Lee, I.W. Kim, J.S. Kim, C.W. Ahn, B.H. Park, Ferroelectric and piezoelectric properties of $Na_{0.52}K_{0.48}NbO_3$ thin films prepared by radio frequency magnetron sputtering, Applied Physics Letters 94 (9) (2009) 092902.
[16] K. Shibata, F. Oka, A. Ohishi, T. Mishima, I. Kanno, Piezoelectric properties of (K,Na)NbO_3 films deposited by RF magnetron sputtering, Applied Physics Express 1 (1) (2008) 011501.
[17] X. Wang, U. Helmersson, S. Olafsson, S. Rudner, L.D. Wernlund, S. Gevorgian, Growth and field dependent dielectric properties of epitaxial $Na_{0.5}K_{0.5}NbO_3$ thin films, Applied Physics Letters 73 (7) (1998) 927–929.

[18] J.G. Wu, J. Wang, Phase transitions and electrical behavior of lead-free $(K_{0.50}Na_{0.50})NbO_3$ thin film, Journal of Applied Physics 106 (6) (2009) 066101.

[19] A. Wold, B. Post, E. Banks, Rare earth nickel oxides, Journal of the American Ceramic Society 79 (18) (1957) 4911–4913.

[20] M.S. Chen, T.B. Wu, J.M. Wu, Effect of textured $LaNiO_3$ electrode on the fatigue improvement of $Pb(Zr_{0.53}Ti_{0.47})O_3$ thin films, Applied Physics Letters 68 (10) (1996) 1430–1432.

[21] H. Han, J. Zhong, S. Kotru, P. Padmini, X.Y. Song, R.K. Pandey, Improved ferroelectric property of $LaNiO_3/Pb(Zr_{0.2}Ti_{0.8})O_3/LaNiO_3$ capacitors prepared by chemical solution deposition on platinized silicon, Applied Physics Letters 88 (9) (2006) 092902.

[22] S.C. Lai, H.-T. Lue, K.Y. Hsieh, S.L. Lung, R. Liu, T.B. Wu, P.P. Donohue, P. Rumsby, Extended-pulse excimer laser annealing of $Pb(Zr_{1-x}Ti_x)O_3$ thin film on $LaNiO_3$ electrode, Journal of Applied Physics 96 (5) (2004) 2779–2784.

[23] G.S. Wang, J.G. Cheng, X.J. Meng, J. Yu, Z.Q. Lai, J. Tang, S.L Guo, J.H. Chu, G. Li, Q.H. Lu, Properties of highly (100) oriented $Ba_{0.9}Sr_{0.1}TiO_3/LaNiO_3$ heterostructures prepared by chemical solution routes, Applied Physics Letters 78 (26) (2001) 4172–4174.

[24] L. Yang, F. Ponchel, G. Wang, D. Remiens, J.-F. Legier, D. Chateigner, X. Dong, Microwave properties of epitaxial (111)-oriented $Ba_{0.6}Sr_{0.4}TiO_3$ thin films on $Al_2O_3(0001)$ up to 40 GHz, Applied Physics Letters 97 (16) (2010) 162909.

[25] X. Lei, D. Rémiens, F. Ponchel, C. Soyer, G. Wang, X. Dong, Optimization of PST thin films grown by sputtering and complete dielectric performance evaluation: an alternative material for tunable devices, Journal of the American Ceramic Society 94 (12) (2011) 4323–4328.